Stockton, G. W., Johnson, K. G., Butler, K. W., Tulloch, A. P., Boulanger, Y., Smith, I. C. P., Davis, J. H., & Bloom, M. (1977) *Nature (London) 269*, 267–268.
Tardieu, A., Luzzati, V., & Reman, F. C. (1973) *J. Mol. Biol. 75*, 711–733.
Warren, G. B., Toon, P. A., Birdsall, N. J. M., Lee, A. G., & Metcalfe, J. C. (1974) *Proc. Natl. Acad. Sci. U.S.A. 71*, 622–626.
Warren, G. B., Houslay, M. D., Metcalfe, J. C., & Birdsall, N. J. M. (1975) *Nature (London) 255*, 684–687.
Worcester, D. L., & Franks, N. P. (1976) *J. Mol. Biol. 100*, 359–378.
Yeagle, P. L., Hutton, W. C., Huang, C.-H., & Martin, R. B. (1975) *Proc. Natl. Acad. Sci. U.S.A. 72*, 3477–3481.

# Physical Studies of Cell Surface and Cell Membrane Structure. Determination of Phospholipid Head Group Organization by Deuterium and Phosphorus Nuclear Magnetic Resonance Spectroscopy†

Robert Skarjune and Eric Oldfield*

ABSTRACT: Phospholipid head group conformations in 1,2-dipalmitoyl-*sn*-glycero-3-phosphocholine (DPPC), 1,2-dipalmitoyl-*sn*-glycero-3-phosphoethanolamine (DPPE), DPPC–cholesterol, and DPPE–cholesterol dispersions, in excess water above the pure lipid gel to liquid-crystal phase transition temperature, have been calculated by using comparisons between experimental $^2H$ and $^{31}P$ NMR spectral parameters and theoretical results obtained from a plausible model of head group motions. The new calculations are compared with results obtained in previous studies [Seelig, J., Gally, H. U., & Wohlgemuth, R. (1977) *Biochim. Biophys. Acta 467*, 109–117; Brown, M. F., & Seelig, J. (1978) *Biochemistry 17*, 381–384; Seelig, J., & Gally, H. U. (1976) *Biochemistry 15*, 5199–5204] and are shown to agree qualitatively under certain highly restrictive conditions. Under more general conditions, it is shown that many possible solutions are generated but that these may often be separated into a small number of likely conformations in which the head group torsion angles are restricted to specific ranges rather than to a discrete set of values. There is no NMR evidence, however, to support the notion that there are only single conformational solutions to the NMR measurements for the above phospholipid systems.

Recent years have witnessed the introduction and use of a wide variety of physical methods for the study of membrane structure, and neutron diffraction (Worcester, 1976) and nuclear magnetic resonance spectroscopy (NMR)[1] (Mantsch et al., 1977; Seelig, 1977) have been especially informative because they can be used to study both structural and motional aspects of model and biological membrane organization. Of course, in order to extract the maximum amount of information from these techniques, it is necessary to interpret the spectroscopic data in terms of either some static or dynamic picture of molecular organization. For NMR spectroscopy, this is frequently a difficult task. Nevertheless, Seelig et al. (1977) recently described a method which uses results from both of the above techniques to formulate models of phospholipid head group motions. These models were tested quantitatively against experimental $^2H$ and $^{31}P$ NMR data, and the results appeared to indicate that, within a limited conformational space, only one set of head group torsion angles was consistent with the NMR parameters found for 1,2-dipalmitoyl-*sn*-glycero-3-phosphocholine (DPPC) in multilamellar dispersions. Similar results were found for 1,2-dipalmitoyl-*sn*-glycero-3-phosphoethanolamine (DPPE) and for DPPC–cholesterol (CHOL) and DPPE–cholesterol systems (Seelig & Gally, 1976; Brown & Seelig, 1978). Recently, Griffin et al. (1978) have performed independent experiments with multidomain samples of DPPC, and their results have yielded the orientation of the phosphate portion of the glycerylphosphorylcholine head group relative to the bilayer normal. The results agree qualitatively with those obtained by Seelig et al. (1977).

In this article we wish to report our own work on assigning feasible conformations to the phospholipid head groups in DPPC, DPPE, DPPC–CHOL, and DPPE–CHOL systems in which we have extended the previous calculations to include a much larger conformational space. We have also examined more closely the relationship between the Griffin and Seelig results. We find that there are exceedingly large numbers of possible head group conformations which can account for the experimental $^2H$ and $^{31}P$ NMR results. There is no evidence to support the notion that there are unique conformational solutions to the NMR data.

## Experimental Section

*Methods.* The model used in these calculations is similar to that described by Seelig and co-workers (Seelig et al., 1977; Seelig & Gally, 1976; Brown & Seelig, 1978). It is derived

† From the Department of Chemistry, University of Illinois at Urbana–Champaign, Urbana, Illinois 61801. *Received April 11, 1979; revised manuscript received August 15, 1979.* This research was supported by the American Heart Association with funds contributed in part by the Illinois Heart Association (Grant 77-1004) and in part by the Illinois Heart Association (Grant N-6) and by the Alfred P. Sloan Foundation.

* Correspondence should be addressed to this author. He is an Alfred P. Sloan Research Fellow, 1978–1980.

[1] Abbreviations used: DPPC, 1,2-dipalmitoyl-*sn*-glycero-3-phosphocholine; DPPE, 1,2-dipalmitoyl-*sn*-glycero-3-phosphoethanolamine; CHOL, cholesterol; NMR, nuclear magnetic resonance.

0006-2960/79/0418-5903$01.00/0 

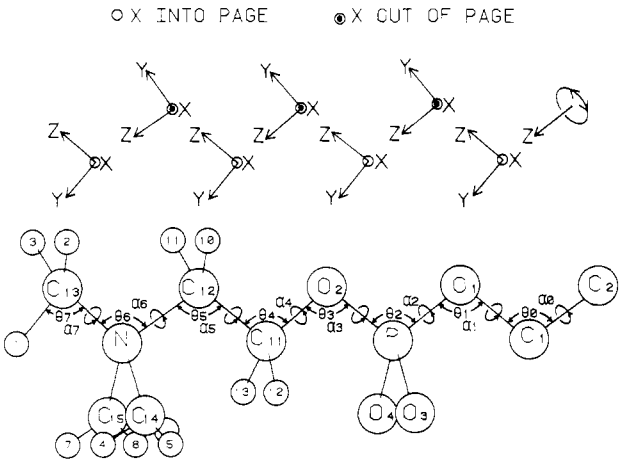


FIGURE 1: All-trans reference conformation for the phosphorylcholine head group. Notation for atoms, bond angles, and torsion angles is according to Sundaralingam (1972). Above each bond segment is the coordinate system for that segment, defined such that the $Z$ axis is parallel to the segment in the indicated direction, the $X$ axis is perpendicular to the plane of the page, and the $Y$ axis is chosen to complete a right-handed Cartesian coordinate system.

Table I: Glycerylphosphorylcholine Bond and Torsion Angles

| bond angle (deg)[a] | torsion angle (deg)[a] |
|---|---|
| $\theta_0 = 108.0$ | $\alpha_0$ = free rotation[b] |
| $\theta_1 = 118.3$ | $\alpha_1 = 345$ (10)[c] |
| $\theta_2 = 103.5$ | $\alpha_2 = 109$ (244)[c] |
| $\theta_3 = 118.6$ | $\alpha_3 = 121$ (244)[c] |
| $\theta_4 = 110.5$ | $\alpha_4 = 42$ (320)[c] |
| $\theta_5 = 114.6$ | $\alpha_5 = 252$ (105)[c] |
| $\theta_6 = 112.7$ | $\alpha_6$ = free rotation[b] |
| $\theta_7 = 109.5$ | $\alpha_7$ = free rotation[b] |

[a] From Sundaralingam (1972). [b] The free rotation for $\alpha_0$, $\alpha_6$, and $\alpha_7$ is assumed in the model used for the calculations. [c] Values in parentheses are for the independent conformer.

from a consideration of results obtained from several physical techniques. Figure 1 shows the all-trans conformation of the glycerylphosphorylcholine group, and this is the arbitrary choice for the reference in these calculations. Table I lists the bond angles and the torsion angles which are appropriate to the calculations. These angles are taken from the crystal structures of glycerylphosphorylcholine (Abrahamsson & Pascher, 1966) and the $CdCl_2$·glycerylphosphorylcholine complex (Sundaralingam & Jensen, 1965). These have been averaged, and the notations given for the atoms, bond angles, and torsion angles are those given by Sundaralingam (1972). Certain assumptions must be made concerning bond angles not given, and we assume here that all H–C–H bond angles are tetrahedral and that the $H_{12}$–$C_{11}$–$H_{13}$ and $H_{10}$–$C_{12}$–$H_{11}$ planes bisect the $\theta_4$ and $\theta_5$ bond angles, respectively. We have defined the reference structure as the conformation in which all torsion angles have the value zero. This differs from Seelig's usage, but the sense of rotation has been preserved; when looking through the axis of rotation, a positive increase is obtained by a clockwise displacement of the farther group. In general, the values of the torsion angles were restricted to a range of 0–360° so that a value of $\alpha$° has a negative of (360 − $\alpha$)°. The few cases where $\alpha > 360°$ represent "wrap-around" to 0° and should cause no confusion.

The crystal studies identify two independent conformers in the glycerylphosphorylcholine unit cell (Abrahamsson & Pascher, 1966). The two structures are related in that each torsion angle in one molecule is approximately the negative of the corresponding torsion angle in the other molecule. The two structures look like mirror images, and they will be referred to as enantiomeric pairs for simplicity.

The motional aspects of the model are derived from several experimental findings. The $C_1$–$C_2$ bond in dilauroylphosphatidylethanolamine has been found to be oriented perpendicular to the bilayer plane in X-ray crystallographic studies (Hitchcock et al., 1974). Furthermore, $^2H$ and $^{31}P$ NMR spectra of oriented lecithin bilayers have been shown to be axially symmetric about the bilayer normal (Stockton et al., 1974; McLaughlin et al., 1975) while the $^{31}P$ chemical shift tensor is axially asymmetric (Griffin et al., 1978). For these reasons, the model incorporates free rotation about the $C_1$–$C_2$ segment. $^2H$ NMR spectra of DPPC bilayers in which $C_1$ has been specifically $^2H$-labeled lead to an order parameter of ~0.66 for this $C_1$–$C_2$ segment (Gally et al., 1975; Seelig & Gally, 1976), so these angular fluctuations are also incorporated into the model.

$^2H$ NMR spectra have been obtained for DPPC specifically labeled at $C_{11}$, $C_{12}$, and the choline methyl groups (Seelig et al., 1977). These results show only one quadrupole splitting for each of the three groups of deuterons. It is difficult to explain this in terms of a static head group structure, and Seelig et al. (1977) have suggested a limited mobility in which the head group undergoes rapid enantiomeric transitions. This kind of motion exchanges the orientations of the deuterons on a given carbon atom, and if the transitions are fast on the NMR time scale only the average orientation is seen, resulting in one quadrupole splitting. The fact that enantiomeric structures are observed in X-ray studies lends additional support to this suggestion. Further, the single methyl deuteron splitting is adequately explained only when free rotation of $\alpha_7$ and $\alpha_6$ is assumed (or, equivalently, a threefold symmetric jump). These motions are also included in the model.

Kohler & Klein (1976) have determined the components and orientation of the chemical shift tensor for phosphorus in DPPC bilayers, obtaining principal values of $\sigma_{11} = -81$ ppm, $\sigma_{22} = -25$ ppm, and $\sigma_{33} = 108$ ppm. Seelig et al. (1977) used this tensor in their choline head group calculations, and we have also used it here. Recently, however, Herzfeld et al. (1978) have revised the orientation and principal components of this tensor, obtaining values of $\sigma_{11} = -81$ ppm, $\sigma_{22} = -25$ ppm, and $\sigma_{33} = 110$ ppm; and we have included additional results incorporating the new tensor for comparison. The orientations are similar with $\sigma_{11}$ and $\sigma_{33}$ nearly parallel to the $O_{11}$–$O_{12}$ vector and the $O_{13}$–$O_{14}$ vector, respectively. $\sigma_{22}$ is chosen to complete a right-handed coordinate system.

A compilation of deuteron quadrupole coupling constants for a range of C–D bonds has shown that 170 kHz is a good average value for paraffinic bonds and that the electric field gradients are very nearly axially symmetric (Seelig, 1977). Exact axial symmetry is assumed here. The axis of symmetry is along the C–D bond and the direction is taken from C to D.

Determination of possible phospholipid head group conformations involves a comparison between experimental and calculated NMR parameters. The experimental data come from $^{31}P$ and $^2H$ NMR experiments with dispersions and oriented bilayers of DPPC, DPPE, specifically deuterated DPPC and DPPE, and these same systems in the presence of cholesterol. For simplicity, we will outline our theoretical methods for the pure DPPC case first. The $^{31}P$ spectra of DPPC in excess water at 49 °C show an axially symmetric "powder pattern" line shape with a breadth ($\Delta\sigma$) of approximately −47 ppm (Gally et al., 1975; Griffin et al., 1976). The $^2H$ spectra of dispersions of specifically $^2H$-labeled DPPC's at the same temperature show quadrupole splittings of ±5900,

Table II: Matrix Elements for the Chain-Segment Transformation Matrix

| | $\hat{X}$ | $\hat{Y}$ | $\hat{Z}$ |
|---|---|---|---|
| $X'$ | $-\cos\alpha$ | $-\cos\theta\sin\alpha$ | $-\sin\theta\sin\alpha$ |
| $Y'$ | $-\sin\alpha$ | $\cos\theta\cos\alpha$ | $\sin\theta\cos\alpha$ |
| $Z'$ | 0 | $\sin\theta$ | $-\cos\theta$ |

±5100, and ±1150 Hz for the $C_{11}$–D, $C_{12}$–D, and methyl deuterons, respectively (Gally et al., 1975). These systems are lamellar liquid crystals, and the NMR parameters are determined by the representations of the appropriate $^2H$ electric field gradient tensors and the phosphorus chemical shift tensor in the coordinate system of the bilayer normal. These tensors are known in their respective principal coordinate systems and must be transformed to the bilayer system. Of course, the transformations are determined by the details of the head group motion, so that the bilayer representations of the tensors include the effects of this motion. The calculated NMR parameters are obtained by mathematically transforming the tensors according to motions assumed in the model. If the calculations yield tensors identical with the experimental tensors, then the particular model is a possible candidate for the real system. We transformed the tensors through successive bonds according to Seelig and co-workers (Seelig et al., 1977; Seelig & Gally, 1976). However, we used a series of four computer programs so that each (beyond the first) could use the previous results to eliminate reexamination of conformational spaces where no solutions existed.

The transformations were done with Cartesian transformation matrices, although Wigner rotation matrices are equally suitable (Rose, 1963). Figure 1 shows the coordinate system for each chain segment in the reference conformation. These are defined according to Flory (1969) with the $X$ axis reversing direction along each successive chain segment. This definition permits the use of the same mathematical form for the transformation matrix for all chain-segment transformations. The coordinate system for the determination of this matrix is shown in Figure 2, and Table II shows the $\hat{X}\hat{Y}\hat{Z} \rightarrow X'Y'Z'$ transformation matrix. Substitution of the proper $\theta$ and $\alpha$ is all that is required for a particular transformation. The transformation is carried out by ordered row–column matrix multiplication according to

$$T' = UT\tilde{U} \tag{1}$$

where $T'$, $T$, $U$, and $\tilde{U}$ are the transformed tensor, original tensor, transformation matrix, and transposed transformation matrix, respectively. We will demonstrate that vector transformations are useful in some cases, and these are defined by

$$V' = UV \tag{2}$$

where $V'$ and $V$ are the transformed and original vectors, respectively, and $U$ is defined above. The calculations were performed by using a CDC Cyber-175 system, and the plotting of solutions was performed with the aid of peripherals described elsewhere (Kang et al., 1979).

The first program determines values of the $\alpha_1$ and $\alpha_2$ torsion angles which satisfy the conditions $-46 \geq \Delta\sigma \geq -48$ ppm. Transformation from the principal axis to the $C_1$–$C_2$ segment is done for both positive and negative torsion angles to account for the enantiomeric transitions. The final transformation is independent of $\alpha_0$, and an analytical expression is easily derived from integration with respect to $\alpha_0$ of the generalized transformation. The two tensors (one each for positive or negative sense of torsion angles) are averaged and then transformed to the bilayer normal system by multiplying each element by

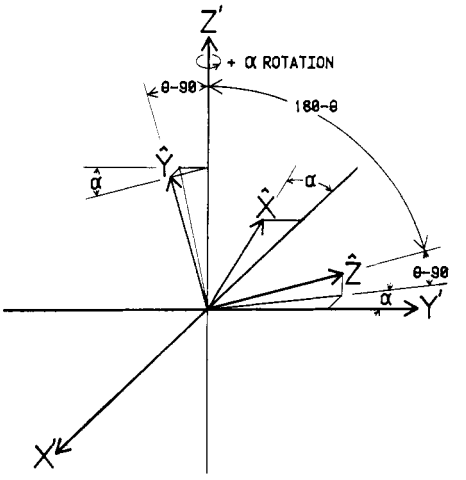


FIGURE 2: Coordinate system for the derivation of the chain-segment transformation matrix. Transformation is from $\hat{X}\hat{Y}\hat{Z}$ to $X'Y'Z'$ with matrix elements listed in Table II.

0.66, which accounts for the $C_1$–$C_2$ segment wobble. The result is obtained from

$$\Delta\sigma = T_{3,3} - T_{2,2} \tag{3}$$

where $T_{3,3}$ and $T_{2,2}$ are the averaged elements in the final tensor (Seelig & Gally, 1976). Of course, the numerical value of the computed $\Delta\sigma$ is a function of the $\alpha_1$ and $\alpha_2$ used for the transformations. Our program increments each torsion angle individually over a specified range, and the calculated $\Delta\sigma$ for each $\alpha_1,\alpha_2$ is compared with the $\Delta\sigma$ obtained from the previous $\alpha_1,\alpha_2$. If $-48 \leq \Delta\sigma \leq -46$ ppm occurs between these two, the program does a linear interpolation to find the approximate $\alpha_1,\alpha_2$ solutions for $\Delta\sigma = -48$ ppm, $\Delta\sigma = -47$ ppm, and $\Delta\sigma = -46$ ppm. Alternatively, if the $\alpha_1,\alpha_2$ pair yields a $\Delta\sigma$ in this range, it is kept as a solution. When the program has completed the torsion angle ranges, the result is the set of $\alpha_1,\alpha_2$ pairs satisfying $-48 \leq \Delta\sigma \leq -46$ ppm within the chosen ranges and with a resolution determined by the increments.

The second program determines values of $\alpha_1$, $\alpha_2$, $\alpha_3$, and $\alpha_4$ which will result in a quadrupole splitting of ±5900 ± 100 Hz for the $C_{11}$ deuterons. The splitting depends on the orientation of the electric field gradient tensor in the coordinate system of the bilayer normal. One tensor is generated for each deuteron, but the enantiomeric pair transitions exchange these orientations, so only the averaged tensor is expressed. The axial symmetry of the tensors in their principal coordinate systems permits some useful simplifications. The symmetry direction of these tensors is along the C–D bond, and we can represent this by a unit vector from $C_{11}$ to D. Proper rotation about the $C_{11}$–$O_2$ segment ($\alpha_4$) will bring either deuteron into a trans-planar conformation with respect to the lower part of the molecule in the reference position (Figure 1). The axial symmetry of the tensor allows an arbitrary choice of the $X$ and $Y$ directions in the $XY$ plane. These are chosen so that, after the $\alpha_4$ rotation, the electric field gradient tensor $X$ axis lies parallel to the $X$ axis of the $C_{12}$–$C_{11}$ segment in the reference conformation. Thus, the initial transformation differs from the chain transformation only in that a new $\theta$ must be determined and the required rotation be included by adding the appropriate bias to the $\alpha_4$ torsion angle. This $\theta$ and bias are determined by using spherical trigonometry and the assumptions contained in the description of the model. An even more useful simplification results from consideration of the transformation of an axially symmetric tensor to an axially symmetric axis, which is the net transformation from principal

coordinate system to bilayer normal. The resultant tensor is

$$\begin{matrix} (1/2)q((3/2)\times \sin^2\theta - 1) & 0 & 0 \\ 0 & (1/2)q((3/2)\times \sin^2\theta - 1) & 0 \\ 0 & 0 & (1/2)q(3\times \cos^2\theta - 1) \end{matrix} \quad (4)$$

where $\theta$ is the angle between the CD vector and the bilayer normal and $q$ is the original $ZZ$ component. This is axially symmetric, as expected, so the tensor may be completely described by giving the orientation and magnitude of the $ZZ$ component. The magnitude is derived from the original $ZZ$ component by multiplication by $(1/2)(3\cos^2\theta - 1)$, and the final orientation is parallel to the bilayer normal. Therefore, it is necessary only to determine the angle between the C–D segment and the bilayer normal, because the magnitude of the original $ZZ$ component is known. This is easily performed by using vector transformations to transform the $\hat{Z}$ vector from the $C_{11}$–D segment, along the chain, to the bilayer normal. The $Z$ component in the bilayer normal representation is the cosine of the angle between the C–D vector and the bilayer normal. Thus, the final $ZZ$ tensor component is given by

$$ZZ_{\text{result}} = ZZ_{\text{original}}[(3/2)Z_{\text{final}}^2 - 1/2]0.66 \quad (5)$$

where $Z_{\text{final}}$ is the final $Z$ vector component and the 0.66 accounts for $C_1$–$C_2$ segment wobble. This is useful because a vector transformation requires fewer computer manipulations. The program transforms the $C_{11}$–$D_{12}$ vector as a function of the chosen torsion angles and their negatives. This results in two $ZZ$ components which are averaged to give the final component. The expected splitting is given by

$$\Delta\nu = (3/4)(ZZ_{\text{final}})eQ/h \quad (6)$$

where $e$, $Q$, and $h$ are, respectively, the elementary electron charge, quadrupole moment of the deuteron, and Planck's constant. In the transformations, $\alpha_3$ and $\alpha_4$ are individually incremented over user defined ranges for each $\alpha_1$,$\alpha_2$ pair generated by the first program. Linear interpolation yields $\alpha_1$, $\alpha_2$, $\alpha_3$, and $\alpha_4$ values for which $\Delta\nu = \pm 5900 \pm 100$ Hz and $-48 \leq \Delta\sigma \leq -46$ ppm.

Next we search for $\alpha_1$, $\alpha_2$, $\alpha_3$, $\alpha_4$, and $\alpha_5$ values which result in $\Delta\nu = \pm 5100 \pm 100$ Hz for the $C_{12}$ deuterons. The program which performs this search is entirely analogous to the previous program. The $C_{12}$–$D_{10}$ vector is transformed to the bilayer normal for a chosen range of $\alpha_5$ values and their negatives. The values of $\alpha_1$, $\alpha_2$, $\alpha_3$, and $\alpha_4$ are taken from solutions from the second program. The expected splitting is calculated, and linear interpolation yields sets of $\alpha_1$, $\alpha_2$, $\alpha_3$, $\alpha_4$, and $\alpha_5$ which satisfy $\Delta\nu(C_{12}D) = \pm 5100 \pm 100$ Hz, $\Delta\nu(C_{11}D) = \pm 5900 \pm 100$ Hz, and $-48 \leq \Delta\sigma \leq -46$ ppm.

For the methyl deuterons, free rotation about $\alpha_6$ and $\alpha_7$ averages the nine electric field gradient tensors into one axially symmetric tensor along the $C_{12}$–N bond. The magnitude of the $ZZ$ resultant is easily obtained by substitution of the two bond angles into the above tensor equations. The coordinate system of the tensor is identical with that of the $C_{12}$N system, so chain transformation matrices are used to transform the $C_{12}$–N unit vector to the bilayer normal. The derived angle is used in addition to factors introduced by $\alpha_6$ and $\alpha_7$ free rotation to calculate the expected splitting. As described before, the transformations are performed for chosen torsion angles and their negatives, but, for the final calculation, all values of $\alpha_1$, $\alpha_2$, $\alpha_3$, $\alpha_4$, and $\alpha_5$ are taken from the solutions generated by the previous program. The calculated splitting for each set of torsion angles is compared with $\Delta\nu = \pm 1150 \pm 100$ Hz, and all sets yielding splittings within this range are considered as possible solutions to the entire glyceryl-phosphorylcholine head group conformation.

It is obvious that the nesting of the computer programs permits efficient searching for solutions. This is important because the calculations require a great deal of computer time, and the extensive looping is quite expensive. Even more important is that our programs effectively test all conformations within the chosen ranges with a resolution determined by the increments. The exact number of solutions generated is somewhat misleading as it depends upon the details of the incrementing and interpolations; however, the degree of confidence placed in any one solution decreases as the total number of solutions increases.

Previous workers (Seelig & Gally, 1976; Brown & Seelig, 1978; Seelig et al., 1977) performed their calculations by first choosing a conformation, near the crystallographic structure, which closely satisfied all the NMR parameters. Each torsion angle was varied over a range defined by the crystallographic value ±30° while holding *all* of the other torsion angles constant. It is clear that this method for varying the torsion angles examines a very limited conformational space. Assuming 2° increments, the previous method would test $30 \times 5$ conformations while our programs effectively test $30^5$ conformations. Of course, these additional conformations do not affect the precision of the solutions but serve to examine a much larger conformational space.

## Results and Discussion

Figure 3A shows our results for torsion angles $\alpha_1$–$\alpha_5$ for DPPC using the Kohler and Klein phosphorus chemical shift tensor orientation, with 2° torsion angle increments and torsion angle ranges within ±40° of the crystallographic values, for one member of the enantiomeric pair. As described above, the solutions are found for the experimentally determined NMR parameters ±100 Hz or ±1 ppm for the deuterium and phosphorus values, respectively. This uncertainty is included because the experimental NMR parameters are subject to phasing and other errors which make the exact values difficult to obtain. We have found, however, that reducing the uncertainty by a factor of 2 results in essentially the same results.

Successive pairs of torsion angles, for DPPC, are plotted in Figure 3A, and each solution is represented by a point. While hundreds of solutions are generated, these tend to form clusters which define continuous subspaces in which solutions exist. This result might be loosely interpreted as defining "quasi-conformations" for which the torsion angles are not unique but are confined to more or less restrictive ranges. A careful analysis with plots for all possible torsion angle pairs yields four quasi-conformations with torsion angle ranges listed in Table III. The magnitude of the individual torsion angle ranges can be understood in part by considering the orientation of the rotational axis with respect to the bilayer normal. For example, with $\alpha_1 \simeq 350°$, the $\alpha_2$ axis lies nearly parallel to the bilayer normal. With this orientation, large $\alpha_2$ changes are required to cause small orientational changes in the remainder of the head group. As a result, $\alpha_2$ is almost freely variable over the ±40° range, requiring only small changes in the other torsion angles to regenerate solutions. On the other hand, the $\alpha_1$ axis lies nearly perpendicular to the bilayer normal so small $\alpha_1$ changes result in relatively large orientational changes in the rest of the head group, effectively restricting permissible $\alpha_1$ values to a small range.

The calculations of previous workers (Seelig et al., 1977) resulted in one solution which is represented by a square in Figure 3A; however, these workers examined a very small conformational space as described above. In order to better compare the results, we have repeated the calculations over

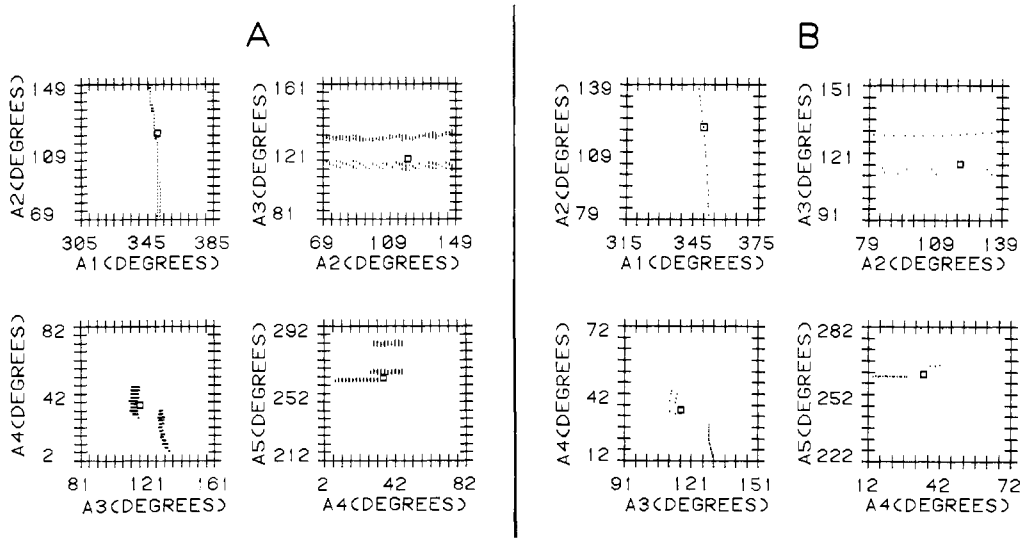


FIGURE 3: Computer-generated conformational solutions for DPPC in excess water at 49 °C using (A) ±40° torsion angle ranges, 2° increments, the tensor of Kohler & Klein (1976), and NMR parameters −48 ppm ≤ $\Delta\sigma$ ≤ −46 ppm, $\Delta\nu_{12,13}$ = ±5900 ± 100 Hz, $\Delta\nu_{10,11}$ = ±5100 ± 100 Hz, and $\Delta\nu_{methyl}$ = ±1150 ± 100 Hz and (B) ±30° torsion angle ranges, 1° increments, the tensor of Kohler & Klein (1976), and the NMR parameters $\Delta\sigma$ = −47 ppm, $\Delta\nu_{12,13}$ = ±5900 Hz, $\Delta\nu_{10,11}$ = ±5100 Hz, and $\Delta\nu_{methyl}$ = ±1150 ± 10 Hz (Seelig et al., 1977). The solution obtained by previous workers (Seelig et al., 1977) is indicated with a square (□).

Table III: Torsion Angle Ranges for Dipalmitoylphosphatidylcholine Head Group Conformers (All Values in Degrees)

| | torsion angle ranges (deg) | | | | |
|---|---|---|---|---|---|
| | $\alpha_1$ | $\alpha_2$ | $\alpha_3$ | $\alpha_4$ | $\alpha_5$ |
| I[a] | 345-353 | 69-149 | 109-114 | 29-46 | 280-284 |
| II[a] | 345-353 | 69-149 | 112-117 | 27-46 | 263-266 |
| III[a] | 345-353 | 69-149 | 126-134 | 8-32 | 259-262 |
| IV[a] | 345-347 | 144-149 | 111-113 | 82 | 220-222 |
| I[b] | 348-352 | 86-134 | 111-113 | 34-43 | 281-282 |
| II[b] | 348-352 | 85-132 | 113-114 | 33-42 | 265-266 |
| III[b] | 347-352 | 79-109 | 128-130 | 14-28 | 260-261 |
| I[c] | 343-347 | 69-149 | 106-113 | 34-56 | 280-284 |
| II[c] | 343-347 | 69-149 | 107-114 | 32-52 | 264-266 |
| III[c] | 343-347 | 69-149 | 122-128 | 12-44 | 259-261 |

[a] DPPC from Figure 3A and additional plots. [b] DPPC from Figure 3B and additional plots. [c] DPPC from Figure 5B and additional plots.

a ±30° space around each torsion angle with 1° increments while searching for the exact NMR parameters, with the exception of the methyl deuteron value which was examined over a ±1150 ± 10 Hz range because of the nature of the computer program. The results in Figure 3B show a similar but less diffuse pattern. Nevertheless, many solutions are generated which can be separated into three slightly better defined quasi-conformations listed in Table III. We have also taken several of these solutions and performed the same type of calculations as the previous workers; in each case, varying only one torsion angle at a time, while holding the others constant at the original value, resulted in only one solution being generated. This is clearly a consequence of the great sensitivity of the NMR parameters to the exact values of the torsion angles. A change of one degree in one torsion angle is sufficient to change one or more NMR parameters to exclude the new conformation as a solution; however, slight adjustment of the other torsion angles may regenerate solutions. As a result, to yield the full information obtainable from the calculations, it is necessary to simultaneously vary all adjustable torsion angles.

This has important consequences in terms of the physical intepretation of the quasi-conformations described above. The

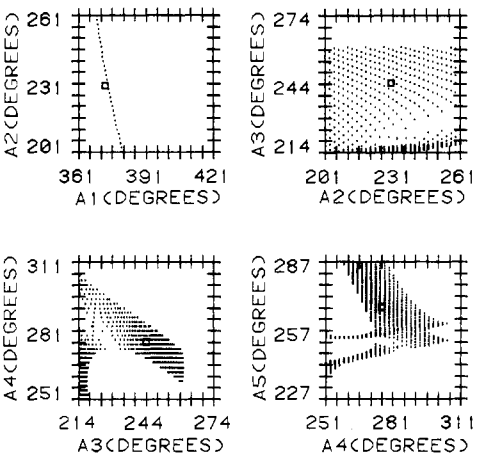


FIGURE 4: Solutions for DPPE in excess water at 49 °C using ±30° torsion angle ranges, 2° increments, the tensor of Kohler & Klein (1976), and the NMR parameters $\Delta\sigma$ = −37.5 ppm, $\Delta\nu_{12,13}$ = ±9700 Hz, and $\Delta\nu_{10,11}$ = ±3700 Hz (Seelig & Gally, 1976) where deuteron notation analogous to that of the choline in Figure 1 has been used for DPPE. The solution obtained by previous workers (Seelig & Gally, 1976) is indicated with a square (□).

torsion angles may not vary freely and independently over the ranges indicated, because cooperative torsion angle changes must occur for a new conformation to remain a solution. Therefore, the quasi-conformations simply restrict the regions where we may find correct solutions.

We have also performed similar calculations for DPPE. The results are shown in Figure 4, by using NMR parameters and X-ray angles determined previously (Seelig & Gally, 1976; Hitchcock et al., 1974; DeTitta & Craven, 1973). The insignificant restriction of the torsion angles is a result of the lack of a methyl deuteron NMR parameter to refine the solutions determined by the third program. We find that the final program decreases the number of solutions generated in the penultimate program by a factor of about 20. Again, previous workers found only one conformation upon examination of a torsion angle space which did not allow simultaneous torsion angle changes (Seelig & Gally, 1976).

Previous workers have also performed calculations for DPPC–cholesterol and DPPE–cholesterol dispersions containing 1:1 molar ratios of lipid to cholesterol (Brown & Seelig,

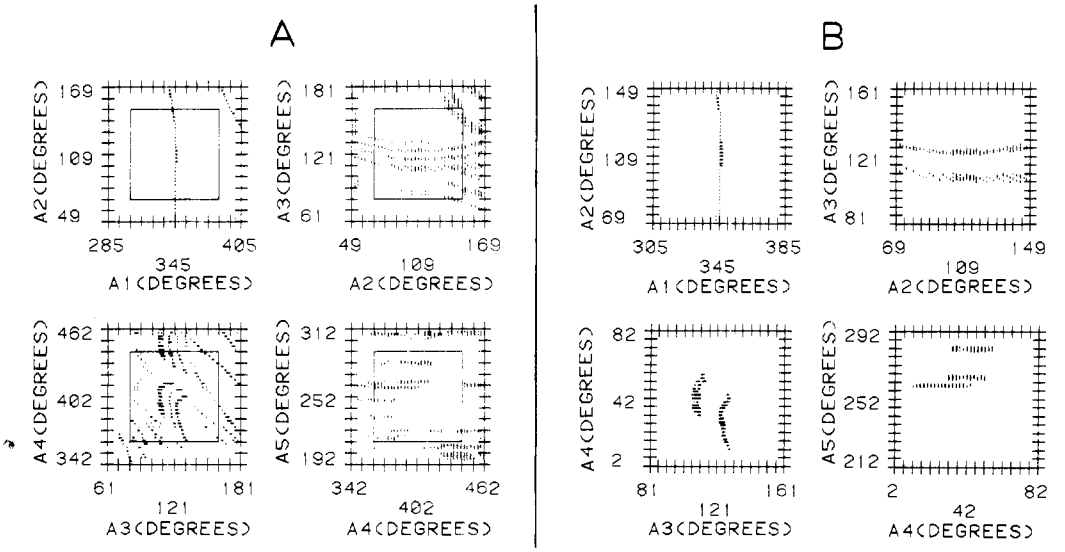


FIGURE 5: Solutions for DPPC in excess water at 49 °C using (A) ±60° and (B) ±40° torsion angle ranges, the tensor of Herzfeld et al. (1978), and the NMR parameters $\Delta\sigma = -47 \pm 1$ ppm, $\Delta\nu_{12,13} = \pm 5900 \pm 100$ Hz, $\Delta\nu_{10,11} = \pm 5100 \pm 100$ Hz, and $\Delta\nu_{methyl} = \pm 1150 \pm 100$ Hz (Seelig et al., 1977). The inner regions in (A) represent ±40° regions with a 3° increment; the outer boundaries are the results of a ±60° 3° increment search. The results of (B) used a 2° increment.

1978). Our results for DPPC–cholesterol indicate a complicated pattern of quasi-conformations. Plots of our DPPE–cholesterol results are similar to our DPPE results and demonstrate no useful restriction of torsion angles. Again, the previous workers found one solution, presumably a result of varying only one torsion angle at a time while holding the others constant at a single value determined to be a solution.

We have also compared our results with those of other workers who have determined the orientation of the phosphate portion of the DPPC head group using an independent method (Griffin et al., 1976, 1978). By examination of the $^{31}P$ NMR spectra of monodomain samples of DPPC monohydrate, it has been determined that the $O_3$–P–$O_4$ plane is oriented at 47 ± 5° with respect to the bilayer normal, and the $ZZ$ component of the phosphorus chemical shift tensor is parallel to the bilayer surface. Other workers (Herzfeld et al., 1978) have refined the orientation of the phosphorus chemical shift tensor in the molecular frame, and we have repeated our DPPC calculations using this new orientation.

To examine some possible relationships between the two independent approaches, we modified our $\alpha_1,\alpha_2$ program to search for $\alpha_1,\alpha_2$ pairs which yielded a 47 ± 5° orientation of the $O_3$–P–$O_4$ plane or a $ZZ$ shift tensor component parallel to the bilayer. We find that no $\alpha_1,\alpha_2$ pair satisfies both orientation conditions and $\Delta\sigma = -47 \pm 1$ ppm. By use of the Kohler and Klein tensor orientation, there are three pairs of regions of intersection, although none of these occur within the ±40° crystallographic regions with respect to $\alpha_2$. One possible explanation might be that enantiomeric transitions are not occurring. However, in this case the Herzfeld orientation yields six intersections which lead to the $C_{11}$ and $C_{12}$ deuterons becoming nonequivalent. A second possibility is that the Herzfeld tensor orientation deviates slightly from the true orientation. The differences between the Herzfeld and the Kohler and Klein orientations are on the order of 10° for each principal axis, so relatively small orientational differences can result in significant changes in the pattern of intersections. Because the tensor orientations are based on model compounds, this possibility appears quite probable. Also, the principal values vary strongly with water content and temperature (Herzfeld et al., 1978), compounding the difficulties of choosing the correct shift tensors for our calculations. The fact that the intersections occur outside of the ±40° crystallographic regions is not a serious problem considering the earlier discussion of the orientation of the $\alpha_2$ axis relative to the bilayer normal. We have also examined the effect of increasing the size of the conformational space by performing calculations using the Herzfeld $^{31}P$ tensor orientation and a ±60° search. This point is rather important, because, in considering a larger conformational space for the calculations, we allow a wider range of compensation of the remaining torsion angles when one is slightly changed. The pattern of solutions becomes quite complicated and does not allow a simple interpretation in terms of quasi-conformations, as shown in Figure 5A. Figure 5B, however, shows the same calculations performed over a ±40° space. Careful analysis of plots of all torsion angle pairs now yields three quasi-conformations and reveals that the new $^{31}P$ shift tensor orientation has led to shifts in the torsion angle ranges which are listed in Table III.

From the previous results it is clear that these calculations are rather limited in their ability to restrict the possible ranges of torsion angles required for a determination of the DPPC head group conformation. In the case of DPPE, the limitations are even more severe. Therefore, at the present time, some caution must be exercised in interpretation of phospholipid head group conformations based solely on $^2H$ and $^{31}P$ NMR data. However, calculations such as these should be quite useful if a few conditions can be met. First, the number of NMR parameters should equal or exceed the number of torsion angles to be defined. The significant differences between the DPPC and the DPPE results show the importance of increasing the number of NMR parameters in the analysis. Second, the orientation of chemical shift tensors in the molecular frame must be known quite accurately as demonstrated by the differences between Figures 3A and 5B. Last, the simultaneous incrementing of *all* adjustable torsion angles is necessary to examine a large conformational space. The usefulness of finding a unique result in a small (single torsion angle search) subspace seems dubious.

With these points in mind, it may be possible to completely analyze phospholipid head group structures by carrying out additional $^{13}C$, $^{14}N$, $^{15}N$, and $^{17}O$ NMR experiments, although the synthetic and NMR aspects of this work appear to be

somewhat daunting at this time. Nevertheless, this type of combined approach may lead to the eventual determination of cell surface structure in intact biological membranes themselves.

References


Abrahamsson, S., & Pascher, I. (1966) *Acta Crystallogr. 21*, 79.

Brown, M. F., & Seelig, J. (1978) *Biochemistry 17*, 381.

DeTitta, G. T., & Craven, B. M. (1973) *Acta Crystallogr., Sect. B 29*, 1354.

Flory, P. J. (1969) *Statistical Mechanics of Chain Molecules*, Interscience, New York.

Gally, H. U., Niederberger, W., & Seelig, J. (1975) *Biochemistry 14*, 3647.

Griffin, R. G., Powers, L., Herzfeld, J., Haberkorn, R., & Pershan, P. S. (1976) *Magn. Reson. Relat. Phenom., Proc. Congr. Ampere, 19th, 1976*, 257.

Griffin, R. G., Powers, L., & Pershan, P. S. (1978) *Biochemistry 17*, 2718.

Herzfeld, J., Griffin, R. G., & Haberkorn, R. A. (1978) *Biochemistry 17*, 2711.

Hitchcock, P. B., Mason, R., Thomas, K. M., & Shipley, G. G. (1974) *Proc. Natl. Acad. Sci. U.S.A. 71*, 3036.

Kang, S. Y., Gutowsky, H. S., Hsung, J.-C., Jacobs, R. E., King, T. E., Rice, D., & Oldfield, E. (1979) *Biochemistry 18*, 3257.

Kohler, S. J., & Klein, M. P. (1976) *Biochemistry 15*, 967.

Mantsch, H. H., Saitô, H., & Smith, I. C. P. (1977) *Prog. Nucl. Magn. Reson. Spectrosc. 11*, 211.

McLaughlin, A. C., Cullis, P. R., Hemminga, M. A., Hoult, D. I., Radda, G. K., Ritchie, G. A., Seeley, P. J., & Richards, R. E. (1975) *FEBS Lett. 57*, 213.

Rose, M. E. (1963) *Elementary Theory of Angular Momentum*, Wiley, New York.

Seelig, J. (1977) *Q. Rev. Biophys. 10*, 353.

Seelig, J., & Gally, H. U. (1976) *Biochemistry 15*, 5199.

Seelig, J., Gally, H. U., & Wohlgemuth, R. (1977) *Biochim. Biophys. Acta 467*, 109.

Stockton, G. W., Polnaszek, C. F., Leitch, L. C., Tulloch, A. P., & Smith, I. C. P. (1974) *Biochem. Biophys. Res. Commun. 60*, 844.

Sundaralingam, M. (1972) *Ann. N.Y. Acad. Sci. 195*, 324.

Sundaralingam, M., & Jensen, L. H. (1965) *Science 150*, 1035.

Worcester, D. L. (1976) *Biol. Membr. 3*, 1.


# Chemical Modification of Arginine at the Active Site of the Bovine Erythrocyte Superoxide Dismutase†

Douglas P. Malinowski and Irwin Fridovich*

ABSTRACT: Several $\alpha,\beta$-diketones inactivated the bovine erythrocyte superoxide dismutase, while modifying 1 arginine residue/subunit. With phenylglyoxal it was shown that the degree of inactivation was a linear function of the extent of arginine modification, to a limit of 1 arginine/subunit, and that arginine modification caused extensive changes in the visible absorbance attributed to the copper at the active site. Butanedione or cyclohexanedione plus borate causes a modification of arginine which is reversible by dialysis. With these reagents it was shown that reversal of arginine modification restored the lost activity. Since this reactivation was seen even when (ethylenedinitrilo)tetraacetic acid was present during dialysis, it follows that copper loss was not a factor in the inactivation which accompanied arginine modification. Analysis of tryptic fragments of cyanogen bromide peptides demonstrated that the essential arginine was no. 141 in the linear sequence. This residue is known, from X-ray crystallography, to lie within 6 Å of the active-site copper. Modification of arginine diminished activity to a limit of 10–20% of the native activity, as measured at pH 7.8. It appears possible that arginine may provide electrostatic attraction for incoming $O_2^-$ or may serve in proton conduction during the second half of the catalytic cycle. Alternately, modification of this arginine may simply distort the ligand field of the Cu(II). Copper- and zinc-containing superoxide dismutases from wheat germ, chicken liver, and several mammalian sources all exhibited comparable sensitivity to arginine-modifying reagents.

Bovine erythrocyte superoxide dismutase catalyzes the reaction $O_2^- + O_2^- + 2H^+ \rightarrow H_2O_2 + O_2$ and does so at a rate close to the diffusion limit, over the entire range of pH from 5 to 10 (Klug et al., 1972; Rotilio et al., 1972). The active site contains copper and zinc in close proximity, as determined by X-ray diffraction analysis (Richardson et al., 1975a,b), and the copper functions in catalysis by alternate reduction and reoxidation during successive encounters with $O_2^-$ (Klug et al., 1973; Fielden et al., 1973). Several other copper proteins have been found devoid of this activity, as is the EDTA–copper complex (Asada et al., 1976; McCord & Fridovich, 1969).

Hydrated Cu(II) is an effective catalyst of $O_2^-$ dismutation, but it loses its activity as the pH is raised to the neutral and weakly alkaline range, due to conversion to $Cu(OH)_2$ (Rabani et al., 1973; Koppenol et al., 1976). If the formation of the hydroxide could somehow be prevented, then free Cu(II) might exhibit an activity comparable to that of the Cu(II) at the active site of the enzyme over a broad range of pH. Even then, one would be hard put to explain the catalytic efficiency of the enzyme, since it has 130 times more surface area than does aquated Cu(II) and random collisions with the protein surface would render most collisions between the enzyme and $O_2^-$ fruitless (Koppenol, 1979). Furthermore, the isoelectric point of BESOD[1] is 5.0 (Bannister et al., 1971) and the protein

†From the Department of Biochemistry, Duke University Medical Center, Durham, North Carolina 27710. *Received August 7, 1979.* This work was supported by research grants from the National Institutes of Health, Bethesda, MD (GM-10287), the U.S. Army Research Office, Research Triangle Park, NC (DRXRO-PR-P-15319-L), and Merck Sharp & Dohme, Rahway, NJ.

0006-2960/79/0418-5909$01.00/0 